Characterization of nuclear wave packets describing molecular photodissociation

M. Lein,[a] M. Erdmann, and V. Engel[b]
Institut für Physikalische Chemie, Am Hubland, 97074 Würzburg, Germany

(Received 24 February 2000; accepted 6 June 2000)

A bound-to-free transition initiated by femtosecond excitation of diatomic molecules results in photofragments with a distribution of kinetic energies. A measurement of the kinetic-energy distribution yields the modulus squared of the asymptotic momentum-space wave packet prepared in the laser excitation process. On the other hand, the coordinate-space density of the wave packet entering the interaction-free region can be determined from pump–probe integrated fluorescence spectroscopy. We provide several numerical examples to show that this information can be used to determine the phase of the asymptotic wave packet so that this particular quantum-mechanical wave function can be characterized completely. To achieve this aim we use an iteration scheme (Gerchberg–Saxton algorithm) which does not require any further information about the system or the laser pulses. © *2000 American Institute of Physics.* [S0021-9606(00)71033-6]

I. INTRODUCTION

Quantum mechanics uses complex-valued wave functions to predict the outcome of measurements. The absolute square of these wave functions is, in favorable cases, directly obtainable from experiment. In the case of molecular spectroscopy, absorption spectra can be related to the nuclear probability density via the so-called *reflection principle*.[1–3] This principle, of course, is not restricted to molecules; for an application to atomic photoionization, see e.g., the paper by Rost.[4] Femtosecond time-resolved photoelectron spectroscopy[5–7] applied to the vibrational motion of diatomic molecules[8–10] is able to map the temporal changes of the spatial probability density.[11,12] The same can also be achieved using time-gated emission spectroscopy[13] or time-resolved kinetic-energy time-of-flight mass spectroscopy.[14]

Recently, much theoretical work has been devoted to find schemes for a complete characterization of wave functions, see e.g., Refs. 15–18. The time-gated emission spectroscopy was applied to construct a vibrational wave packet moving in a harmonic potential,[19] and recently a sophisticated experiment was performed which showed that it is possible to determine the complex phases of wave packets prepared in atomic cesium.[20]

The purpose of the present paper is to introduce a spectroscopic scheme to find a complex-valued wave function without a detailed knowledge about the system under investigation and the employed excitation pulses. Here the case of femtosecond-pulse induced photofragmentation of a diatomic molecule is considered. Two different experiments are necessary to obtain data which then enter in the theoretical analysis: Firstly, the kinetic-energy distribution of the fragments has to be determined; secondly, a fluorescence signal from one of the atomic fragments as a function of the delay time between two ultrashort laser pulses has to be recorded. These measurements yield the fragment wave-packets in momentum and coordinate space, respectively. Pauli was the first to pose the question, if the knowledge of the coordinate and momentum densities provides sufficient information to determine the wave function completely.[21] From a mathematical point of view it is easy to construct sets of functions which do have the same densities in both Fourier spaces but clearly have a nontrivial phase difference. However, as we will show below, such so-called Pauli-twins most likely do not occur in our case.

The ''phase-retrieval'' problem discussed above has been extensively discussed in microscopy where intensity distributions in image and diffraction plane serve as a starting point.[22–25] Below we employ an iterative scheme which was originally proposed by Gerchberg and Saxton[22] to determine the wave function.

The paper is organized as follows: Section II contains the theory describing the construction of the wave functions. In particular we discuss how the coordinate- and momentum-space densities can be measured and outline the Gerchberg–Saxton algorithm. Numerical results are described in Sec. III. Section IV contains a summary.

II. THEORY

In this paper we treat the photodissociation of diatomic molecules AB, which is initiated by the interaction with a femtosecond laser pulse (the pump pulse). The excitation scheme is displayed in Fig. 1: Initially, all molecules are in the electronic ground state. Photon absorption prepares an ensemble of molecules in an excited electronic state with (in this case) a purely repulsive potential-energy curve $V(R)$, where R denotes the AB interatomic distance. Due to the broad spectral width of the ultrashort laser pulse, a coherent superposition of continuum states is prepared. This wave

[a]Also at: Institut für Theoretische Physik, Am Hubland, 97074 Würzburg, Germany.
[b]Electronic mail: voen@phys-chemie.uni-wuerzburg.de

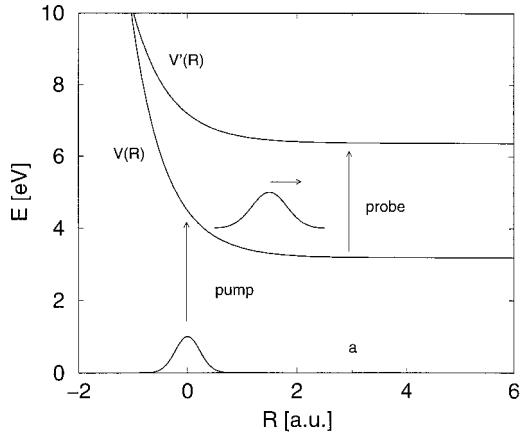

FIG. 1. Excitation scheme for a bound-to-free transition in a diatomic molecule AB. Starting from the vibronic ground state, femtosecond excitation produces photofragments in an excited electronic state with potential curve $V(R)$, where R denotes the AB separation. Also shown is the potential curve $V'(R)$ of another excited state which can be populated by interaction with a time-delayed probe pulse. a denotes the beginning of the Franck–Condon window, where resonant fragment detection can occur.

packet $|\psi(t)\rangle$ then moves into the asymptotic region so that atomic fragments are created with a distribution of kinetic energies. The fragment momentum distribution $\rho(P)$ is the projection of the wave packet on momentum eigenstates $|P\rangle$ with relative kinetic energies $E_P=P^2/(2m)$, m being the reduced mass of the AB system

$$\rho(P)=\lim_{t\to\infty}|\langle P|\psi(t)\rangle|^2=\lim_{t\to\infty}|\psi(P,t)|^2. \tag{1}$$

Thus $\rho(P)$ equals the absolute square of the momentum-space wave function. This distribution can be determined by a kinetic-energy time-of-flight (KETOF) measurement.[14] Owing to the limited experimental resolution, the signal is of the form

$$I(P)=\int dP' g(P,P')\rho(P'), \tag{2}$$

where $g(P,P')$ is an apparatus function. In our numerical examples presented in Sec. III we use a Gaussian

$$g(P,P')=\beta e^{-\pi\beta^2(P-P')^2}. \tag{3}$$

The parameter β determines the width of the detector function. In the limit of large β, $g(P,P')$ becomes a δ-function which corresponds to infinitely high resolution.

Figure 1 contains the potential-energy curve $V'(R)$ of another excited electronic state. The latter can be populated by using a second ultrashort laser pulse (probe pulse) which is time-delayed with respect to the pump pulse. In the case that the carrier frequency of the probe pulse is tuned to an atomic transition (in either A or B), the upper state will be populated if the spatial wave packet $\psi(R,t)$ enters the asymptotic region where resonant excitation is possible. The total fluorescence from the upper electronic state, recorded as a function of the delay time τ between the two laser pulses, can serve as a pump–probe signal $F(\tau)$. Such signals show a typical steplike increase from zero (the wave packet is still located in the interaction region) to a constant (the packet is completely located in the asymptotic region).[26,27]

For a time t_0 not too long after the time when the wave packet is entering the asymptotic region, the spatial density $\rho(R)\equiv\rho(R,t_0)=|\psi(R,t_0)|^2$ can be obtained from the integrated pump–probe fluorescence signal in the case of fragment detection.[28] The main idea for this wave-packet mapping is as follows. The signal monitors the motion of the prepared wave packet into the asymptotic region. The spatial window (Franck–Condon window) where the excitation is effective, ideally starts at a well-defined interatomic distance a (see Fig. 1). Naturally, owing to the spectral width of the pulse, the distance a is only defined approximately. It can be shown that the time-derivative of $F(\tau)$ is proportional to the probability-density flux through a. Relating the flux to $\rho(R,t)$ one finds that, to a very good approximation, the time-derivative of the pump–probe signal is proportional to the density

$$\frac{dF(\tau)}{d\tau}\sim\rho(R,\tau)|_{R=a}. \tag{4}$$

If furthermore the mean speed of the outgoing wave packet is known, the density at $R=a$ can be transformed to obtain the spatial density as a function of R. As a result, the pump–probe signal for fragment detection can be converted to the modulus squared of the R-dependent wave packet.

Again, the experimental resolution has to be taken into account so that the coordinate-space density obtained from the data is of the form

$$I(R)=\int dR' f(R,R')\rho(R'), \tag{5}$$

where the function $f(R,R')$ contains all sources of experimental uncertainties.

The momentum-space density is measured in the limit of long times, but $\rho(P,t)$ remains unchanged while the wave packet moves through the region where the potential $V(R)$ is constant. Hence we can think of the measured $\rho(P)$ and $\rho(R)$ as belonging to the same time t_0, the time when $\psi(R)\equiv\psi(R,t_0)$ and $\psi(P)\equiv\psi(P,t_0)$ have just entered the asymptotic region.

It is worthwhile to mention, that the measurement of the KETOF spectrum is not the only possible experimental method to obtain the momentum-space density. Assuming a weak pump pulse, the state prepared in the pump process can be written as (ignoring unimportant constants)

$$|\psi(t)\rangle=\int_{-\infty}^{t}dt' U(t-t')W(t')\mu|0\rangle. \tag{6}$$

Here $|0\rangle$ is the initial state with energy $E_0=0$, μ denotes the transition dipole moment and $W(t)$ describes the temporal variation of the laser field. $U(t)$ is the propagator for the nuclear motion in the excited electronic state. Projection onto the scattering states $|P-\rangle$ of energy E_P yields, for times t after the pump excitation is finished,[29] the expression

$$\langle P-|\psi(t)\rangle=e^{-iE_Pt}\langle P-|\mu|0\rangle I(E_P), \tag{7}$$

with the integral

$$I(E_P)=\int_{-\infty}^{+\infty} dt' W(t') e^{iE_P t'}. \tag{8}$$

Here we used the fact that, if the pump pulse has decayed to zero, the upper limit of the time-integral may be extended to infinity.

We now concentrate on a time t_0 where the state $|\psi(t)\rangle$ is completely localized in the asymptotic region. Inserting the definition of $|P-\rangle$ in terms of the Møller operator Ω_-[30] one finds

$$\langle P-|\psi(t_0\rangle=\langle\Omega_- P|\psi(t_0)\rangle=\langle P|\Omega_-^\dagger \psi(t_0)\rangle, \tag{9}$$

where

$$\Omega_-^\dagger=\lim_{t\to+\infty} U_0^\dagger(t)U(t), \tag{10}$$

and $U_0(t)$ is the free-particle propagator. Since $|\psi(t_0)\rangle$ is localized in the interaction-free region the propagator $U(t)$ equals $U_0(t)$ so that in the above scalar product $\Omega_-^\dagger$ is the unit operator. Noting furthermore that $|\langle P-|\mu|\psi_0\rangle|^2$ is proportional to the absorption cross section[3] $\sigma(E_P)$ we finally find the asymptotic momentum distribution

$$|(P|\psi(t_0)\rangle|^2=|\psi(P,t_0)|^2\sim\sigma(E_P)|I(E_P)|^2. \tag{11}$$

The last equation relates the momentum-space density to the product of the absorption cross section and the spectral distribution of the pump pulse. Thus a measurement of $\sigma(E_P)$ can provide the momentum distribution if the employed laser pulse is well characterized.

The experiments described above allow, at least in principle, for a determination of the densities $\rho(P)=|\psi(P)|^2$ and $\rho(R)=|\psi(R)|^2$. We now pose the following question, as it was first done by Pauli:[21] If the momentum-space and coordinate-space densities are determined to a sufficiently high accuracy, does this provide us with enough knowledge to determine the complex-valued wave function? It is immediately clear that two wave functions $\psi(R)$ and $e^{i\phi}\psi(R)$ have the same densities if ϕ is a constant, i.e., the sole knowledge of the densities does not fix the overall phase, which is, however, irrelevant in quantum mechanics. Besides from that, wave functions with non-trivial phase difference can also yield identical densities.[23,24] It has been shown that,[24] using the definition

$$\psi(R)=\int_{-\beta}^{\beta} \frac{dP}{2\pi}\psi(P)e^{iPR}, \tag{12}$$

the problem has a unique solution (up to an overall phase factor) if the following conditions hold:

(i) $\psi(P)$ is a holomorphic function of P,
(ii) $\psi(P=\beta)\psi^*(P=-\beta)\neq 0$,
(iii) $|\psi(P=\beta)|^2\neq|\psi(P=-\beta)|^2$.

Physically, we know that the asymptotic momentum-space wave function can be expanded in a set of plane waves which are analytic functions, so that (i) is fulfilled. Condition (ii) is merely a mathematical requirement necessary to carry out the mathematical proof as given in Ref. 24. Since in our numerical calculation the wave functions are never exactly zero at the grid boundaries we may regard (ii) to be fulfilled as well. Finally, condition (iii) means that the entering density does not strictly assume the same value at the boundaries. This is unlikely in our case since the fragmentation dynamics in general produces an asymmetrical momentum distribution. Therefore, (iii) is usually fulfilled.

Of course one might argue that the computer, which is provided with a discrete set of data, cannot distinguish between an analytical or nonanalytical solution.[24] Nonanalytical solutions are not physically reasonable and one should be able to reject them on physical grounds. In our numerical examples we did always find converged solutions which matched the exact ones.

We will now describe an iterative scheme to find the complex-valued wave function from the known densities. The scheme was first used in microscopy and is known as Gerchberg–Saxton algorithm.[22] Denoting the experimentally determined functions as $a(P)=\sqrt{I(P)}$ and $a(R)=\sqrt{I(R)}$, the scheme is started as (equivalently the momentum-space density could serve as starting point)

$$\psi_0(R)=a(R), \tag{13}$$

and the Fourier transform of this function yields $\psi_0(P)$. Next we calculate

$$\psi_1(P)=a(P)\frac{\psi_0(P)}{|\psi_0(P)|}. \tag{14}$$

Taking the Fourier transform yields $\psi_1(R)$ which is used to calculate

$$\psi_2(R)=a(R)\frac{\psi_1(R)}{|\psi_1(R)|}. \tag{15}$$

This iteration scheme may be continued until convergence is achieved. A measure for the deviation of the iterated coordinate-space amplitude from the exact one is given by

$$\delta_n=\int dR\{|\psi(R)|-|\psi_n(R)|\}^2. \tag{16}$$

Gerchberg and Saxton have shown[22] that the iteration is stable in the sense that δ_n cannot increase with increasing n (considering only odd n because for even n, δ_n equals zero by construction).

III. RESULTS

Although we have discussed the dissociation of a diatomic molecule in the preceding sections, we will first use a model which was designed to describe the dissociation of a triatomic molecule in our numerical examples. Nevertheless, since this model is one-dimensional it is generic to describe an AB fragmentation process. The potential-energy curves displayed in Fig. 1 were employed[31] to describe the first gas-phase femtosecond experiments investigating the dissociation of the ICN molecule.[32] Here R denotes the I–CN relative distance, where the value of zero corresponds to the equilibrium distance of the molecule in its electronic ground state. The reduced mass of the I+CN system was used in our calculation.

Let us first regard the femtosecond excitation with a single Gaussian pulse of 30 fs width (full width at half maxi-

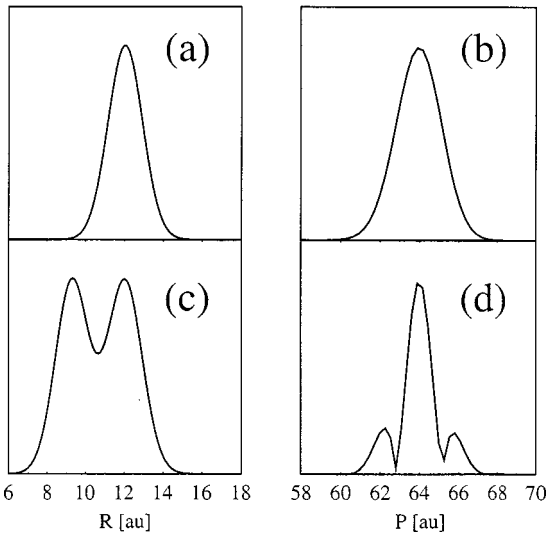

FIG. 2. Modulus of the coordinate-space (a) and momentum-space (b) wave function resulting from the interaction with a 30 fs pump pulse. (c) and (d): Same as (a) and (b) but for a pump pulse consisting of two 30 fs pulses which are time-delayed by 40 fs.

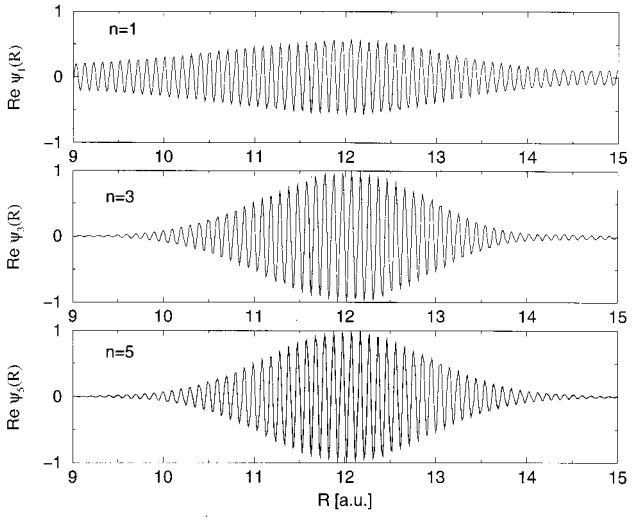

FIG. 3. Iteration of the wave function with input densities as displayed in Figs. 2(a) and 2(b). Shown are the real parts of the iterated wave functions $\psi_n(R)$ obtained after n iteration steps, as indicated. The lower panel additionally contains the numerically exact wave function.

mum). Details of the calculation, which was performed within time-dependent perturbation theory, can be found elsewhere.[28] In the latter work it was also described in detail how to construct the coordinate density $\rho(R)$ which is displayed in Fig. 2(a) together with the corresponding momentum density $\rho(P)$ [Fig. 2(b)]. The densities were calculated at a time of 190 fs after the maximum of the Gaussian-shaped pump pulse. At this time, the wave packet is already localized in the asymptotic region.

We also calculated wave functions for a pump excitation with a pulse envelope consisting of the sum of two Gaussians of 30 fs width, which are delayed to each other by $T=40$ fs. This results in the coordinate-space wave packet as displayed in Fig. 2(c). Here the momentum-space density exhibits a characteristic structure [Fig. 2(d)] which can be understood as follows: Two wave packets $|\varphi(t)\rangle$ and $|\varphi(t-T)\rangle$ are created by identical but delayed pulses; the asymptotic fragment distribution then is

$$\rho(P)=\lim_{t\to\infty}|\langle P|(|\varphi(t)\rangle+|\varphi(t-T)\rangle)|^2. \tag{17}$$

This expression can be evaluated in momentum space as

$$\rho(P)=|\varphi(P)|^2\{2+2\cos(E_P T)\}. \tag{18}$$

Thus $\rho(P)$ contains an interference term causing the structure seen in Fig. 2(d). This is analogous to a two-slit experiment; in our case the separation of the slits corresponds to the pulse-delay T.[33]

Using the densities displayed in Figs. 2(a) and 2(b) as input in the Gerchberg–Saxton algorithm we arrived at the functions displayed in Fig. 3. The figure contains the real parts of the spatial wave functions obtained after n iterations. In the lower panel ($n=5$) the real part of the numerically exact wave function (the target wave function) is also plotted. It is nearly identical with the iterated function. Of course, the functions will, in general, differ by an overall phase factor which we eliminated by fixing the phase of both functions to be the same at a particular value of R. We note that the imaginary part of the wave functions shows a similar convergence behavior.

Applying the procedure to the second example [see Figs. 2(c) and 2(d)] yields the real parts of the $\psi_n(R)$ as displayed in Fig. 4. The lower panel compares the exact wave function with the iterated one. Again, an almost perfect agreement is found. The deviation becomes smaller if more iteration steps are performed.

In the above examples we assumed the ideal case that the experimentally determined densities were measured with infinitely high resolution. To investigate the effect of a limited resolution, let us assume that the momentum-space density was obtained using a filter function [Eq. (3)] with a width (full width at half maximum) of 0.83 a.u. In what follows we regard our second example of two-pulse pump

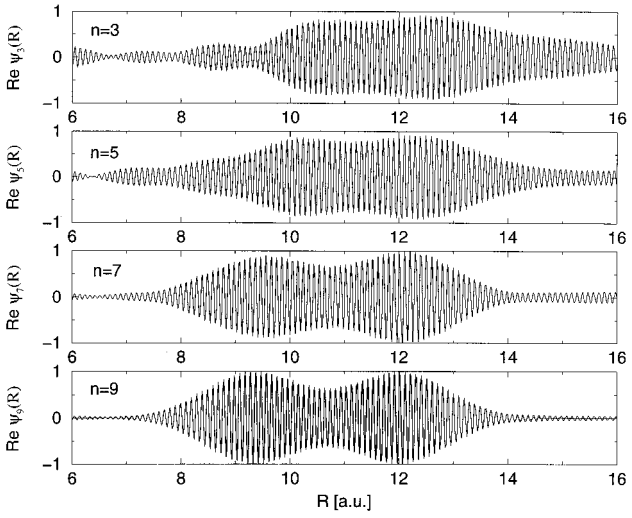

FIG. 4. Same as Fig. 3 but for the two-pulse pump excitation resulting in the densities of Figs. 2(c) and 2(d).

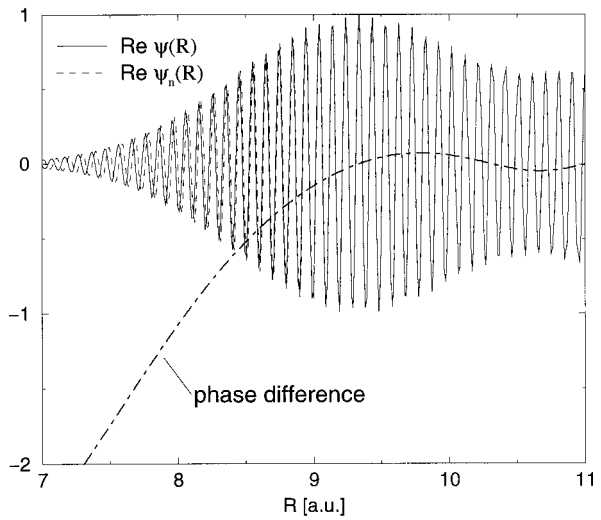

FIG. 5. Real part of the exact (full line) and iterated (dashed line) wave function obtained in the case that the input momentum density is measured with a limited resolution. Also shown is the phase difference between the two functions.

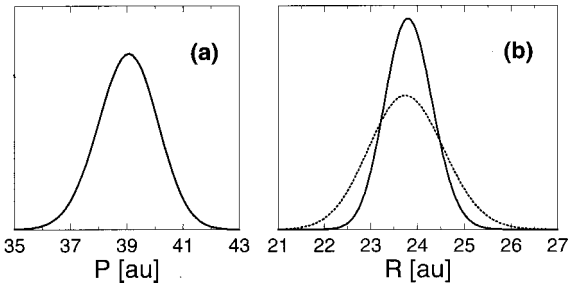

FIG. 6. (a) Momentum-space densities for fragments obtained after femtosecond excitation of I_2 molecules into the B-state dissociation continuum (laser pulse width: 125 fs). Here the case of excitation with an up-chirped or a down-chirped pulse result in almost identical distributions. (b) Coordinate-space densities for up-chirp (solid line) and down-chirp (dotted line) excitation.

excitation, as discussed above. Before examining the results of the numerical iteration we have to note that the problem now is ill-defined: Here we use an input consisting of two densities belonging to functions which are not a pair of Fourier transforms. This leads to a nonconvergent series $\{\psi_1,\psi_2,\psi_3,\ldots\}$. Yet, we find that the series $\{\psi_1,\psi_3,\psi_5,\ldots\}$ converges as well as the series $\{\psi_0,\psi_2,\psi_4,\ldots\}$. Consequently, by construction of the iteration, the difference between $\psi_n(R)$ and $\psi_{n+1}(r), n\gg 1$, is not in the phase but only in the modulus. We choose $\psi_n(R)$ with even n for comparison with the target function because these $\psi_n(R)$ have the correct modulus by construction. Figure 5 compares the real part of the iterated wave function $[\psi_n(R), n=40]$ and exact wave function $\psi(R)$. Also shown is the phase difference calculated as $\Delta S(R)=\ln(\psi/\psi_n)/i$. The phase of the two functions was fixed to be the same at a distance of about 9.5 a.u. [maximum of $|\psi(R)|$]. The plot shows that over a large interval the functions agree very well. Nevertheless deviations are found which is to be expected. As a result we conclude that even in this unfavorable example the output of the iteration compares well with the exact function.

Let us consider another numerical example. Femtosecond excitation of the I_2 molecule from its electronic ground state to the excited *B*-state using a pulse with a wavelength of 490 nm, results in almost complete fragmentation. This is due to the large excitation energy which prepares a superposition of eigenstates with energies in the *B*-state dissociation continuum.[34]

We calculated the *B*-state fragment wave functions using pulses of the form

$$E(t)=e^{-\alpha(t-t_0)^2}e^{-i(\omega(t-t_0)\pm\gamma(t-t_0)^2)}. \tag{19}$$

Here α was chosen such that the Gaussian-shaped function has a width of 125 fs, t_0 was 250 fs and ω corresponded to a wavelength of 490 nm. The field $E(t)$ contains a chirp parameter which was set to $\gamma=5\times10^{-8}$. Two cases were treated: An up-chirp and a down-chirp, corresponding to the plus (minus) sign preceding γ. In the calculation we employed the $v''=1$ vibrational wave function in the electronic ground state as initial wave function. The rotational degree of freedom was ignored.

Figure 6 contains the coordinate- and momentum-space densities which result from the above described excitation. It is interesting to note that the up- and down-chirp excitations yield almost identical momentum-space densities. On the contrary, the coordinate densities differ essentially, here the down-chirp excitation yields a far broader function. This can be understood as follows: For an up-chirp pulse, the parts of the excited-state wave-packet belonging to higher energies, are produced towards the end of the pulse. Since they move outward faster than the low-energy components produced earlier, they catch up with the latter and the resulting wave packet becomes comparatively localized at the time it enters the asymptotic region. On the other hand, down-chirp excitation produces the fast components earlier and the slow ones at the end of the pulse; thus the outmoving packet is spread essentially.

In both cases we found that the Gerchberg–Saxton algorithm converges to the exact complex-valued wave function (not shown). However, we note that the convergence of the algorithm depends on the initial wave function. This is demonstrated in Fig. 7 which, for odd *n*, shows the overall deviation δ_n, see Eq. (16). Using the initial function as defined by Eq. (13), it can be taken from the figure that in either case (up- and down-chirp) the deviation decreases to zero within the first 50 iteration steps. On the other hand, if we use the initial function $\psi_0(R)=a(R)e^{iP_0R}$ (P_0 being the maximum of the momentum distribution) δ_n settles to a constant different from zero (shown is the case of up-chirp excitation). Here the correct phase cannot be obtained. From a practical point of view it means that the numerical iteration has to be performed using several initial trial functions until indeed the function δ_n approaches zero with increasing *n*.

IV. SUMMARY

We have shown that it is, in principle, possible to construct complex-valued wave packets describing photofragments produced through short-pulse excitation. This requires the experimental determination of the fragment kinetic-

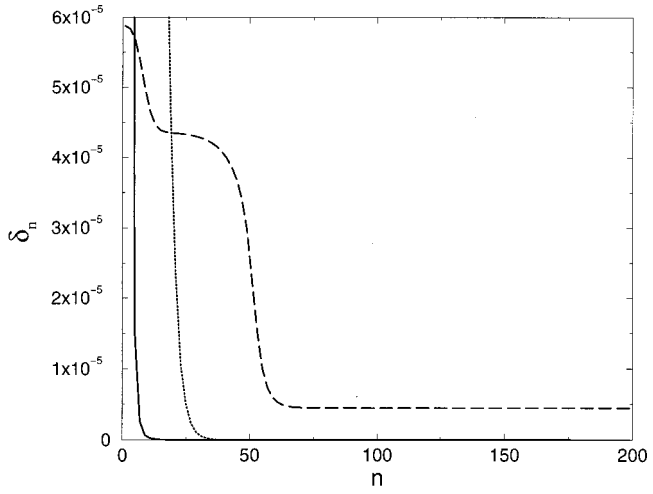

FIG. 7. Convergence behavior of the Gerchberg–Saxton algorithm. Shown is the mean deviation of the iterated coordinate-space amplitude from the exact one, as defined in Eq. (16). Solid and dashed line: Up-chirp excitation; dotted line: Down-chirp excitation. Depending on the initial condition, the deviation tends to zero (convergence and phase retrieval) or a constant (no convergence), see text.

energy distribution and a pump–probe signal detecting the products. These sets of data yield the wave-packet densities in momentum and coordinate space. The phases of the wave function can be obtained from an iteration scheme. By investigating several examples we have shown that the algorithm indeed works excellent, even in unfavorable cases. In the future it would be worthwhile to apply the inversion procedure using the results of an actual experiment, taking all experimental limitations into account.

ACKNOWLEDGMENTS

Financial support from the Deutsche Forschungsgemeinschaft (Schwerpunktprogramm ''Time-dependent phenomena and methods in quantum systems of physics and chemistry,'' project EN 241/6-2) and the Fonds der Chemischen Industrie is gratefully acknowledged. We thank C. Meier for helpful discussions, and M. Freyberger and W. P. Schleich for their stimulating comments on the principles of phase-reconstruction.

[1] G. Herzberg, *Molecular Spectra and Molecular Structure (I), Spectra of Diatomic Molecules* (Van Nostrand, New York, 1950).
[2] J. Tellinghuisen, in *Photodissociation and Photoionization*, edited by K. P. Lawley (Wiley, New York, 1985).
[3] R. Schinke, *Photodissociation Dynamics* (Cambridge University Press, Cambridge, 1993).
[4] J. M. Rost, J. Phys. B: At. Mol. Opt. Phys. **28**, L601 (1995).
[5] M. Seel and W. Domcke, Chem. Phys. **151**, 59 (1991).
[6] M. Seel and W. Domcke, J. Chem. Phys. **95**, 7806 (1991).
[7] W. Domcke and G. Stock, Adv. Chem. Phys. **100**, 1 (1997).
[8] Ch. Meier and V. Engel, Chem. Phys. Lett. **212**, 691 (1993).
[9] Ch. Meier and V. Engel, J. Chem. Phys. **101**, 2673 (1994).
[10] Y. Arasaki, K. Takatsuka, K. Wang, and V. McKoy, Chem. Phys. Lett. **302**, 363 (1999).
[11] A. Assion, M. Geisler, J. Helbing, V. Seyfried, and T. Baumert, Phys. Rev. A **54**, R4605 (1996).
[12] T. Frohnmeyer, M. Hofmann, M. Strehle, and T. Baumert, Chem. Phys. Lett. **312**, 447 (1999).
[13] T. J. Dunn, J. N. Sweetser, I. A. Walmsley, and C. Radzewicz, Phys. Rev. Lett. **70**, 3388 (1993).
[14] A. Assion, T. Baumert, M. Geisler, V. Seyfried, and G. Gerber, Eur. Phys. J. D **4**, 145 (1998).
[15] U. Leonard and M. G. Raymer, Phys. Rev. Lett. **76**, 1985 (1995).
[16] X. Chen and J. A. Yeazell, Phys. Rev. A **56**, 2316 (1997).
[17] C. Leichtle, W. P. Schleich, I. Sh. Averbukh, and M. Shapiro, Phys. Rev. Lett. **80**, 1418 (1998).
[18] W. P. Schleich and M. Raymer, J. Mod. Opt. **44**, No. 11/12 (1997).
[19] T. J. Dunn, I. A. Walmsley, and S. Mukamel, Phys. Rev. Lett. **74**, 884 (1995).
[20] T. C. Winacht, J. Ahn, and P. H. Bucksbaum, Phys. Rev. Lett. **80**, 5508 (1998).
[21] W. Pauli, in *Handbuch der Physik, Vol. XXIV* (Springer, Berlin, 1933).
[22] R. W. Gerchberg and W. O. Saxton, Optik (Stuttgart) **35**, 237 (1972).
[23] P. Schiske, Optik (Stuttgart) **40**, 261 (1973).
[24] A. M. J. Huiser, A. J. J. Drenth, and H. A. Ferwerda, Optik (Stuttgart) **45**, 303 (1976).
[25] G. Yang, B. Dong, B. Gu, J. Zhuang, and O. K. Ersoy, Appl. Opt. **33**, 209 (1994).
[26] N. E. Henriksen, Adv. Chem. Phys. **91**, 433 (1995).
[27] L. W. Ungar and J. A. Cina, Adv. Chem. Phys. **100**, 171 (1997).
[28] V. Engel and N. E. Henriksen, J. Chem. Phys. **112**, 106 (2000).
[29] N. E. Henriksen, Comments At. Mol. Phys. **21**, 153 (1988).
[30] J. R. Taylor, *Scattering Theory: The Quantum Theory on Nonrelativistic Collisions* (Wiley, New York, 1972).
[31] S. O. Williams and D. G. Imre, J. Phys. Chem. **92**, 6648 (1988).
[32] M. Dantus, M. J. Rosker, and A. H. Zewail, J. Chem. Phys. **87**, 2395 (1987).
[33] C. Meier and V. Engel, Phys. Rev. Lett. **73**, 3207 (1994).
[34] C. Wan, M. Gupta, J. S. Baskin, Z. H. Kim, and A. H. Zewail, J. Chem. Phys. **106**, 4353 (1997).